J|A|C|S
COMMUNICATIONS

Published on Web 10/14/2006

# Effect of Nanoscale Geometry on Molecular Conformation: Vibrational Sum-Frequency Generation of Alkanethiols on Gold Nanoparticles

Champika Weeraman, Achani K. Yatawara, Andrey N. Bordenyuk, and Alexander V. Benderskii*

*Department of Chemistry, Wayne State University, Detroit, Michigan 48202*

Received August 8, 2006; E-mail: alex@chem.wayne.edu

Many emerging applications of nanoparticles and nanostructures involve organic molecules chemi- or physisorbed at their surfaces. Conformation of adsorbed molecules often determines the physical, chemical, and biological properties. Activity of catalysts and environmental reactivity of aerosols are other examples where molecular conformation at nanosurfaces plays an important role. As the nanostructures approach the molecular scale, the conformation of molecules adsorbed at their surface will inevitably be influenced by the nanoscale geometry. Here, we investigate the nanoscale geometric effects in a simple model system of (approximately) spherical gold nanoparticles of varying diameter approaching the size of the dodecanethiol adsorbate, ~1.6 nm chain length.

Vibrational spectroscopy in general is a sensitive probe of molecular conformation. However, linear techniques such as Fourier transform infrared (FTIR) absorption and spontaneous Raman spectroscopy are often limited by the spectroscopic selection rules and averaging over the isotropic orientational distribution, which tend to mask the conformational changes. In this paper, we apply nonlinear surface-selective vibrational sum frequency generation (SFG) spectroscopy to characterize the conformation of dodecanethiol on gold nanoparticle surfaces.

Because SFG is a second order nonlinear optical process, it is electric dipole forbidden in systems with inversion symmetry. This results in the well-known surface selectivity of SFG.[1] Another consequence is a propensity rule in the SFG spectroscopy of long alkane chains: all trans (zigzag) conformation usually shows very weak $CH_2$ transitions which effectively cancel one another because of the approximate inversion symmetry.[2,3] Thus the lone terminal $CH_3$ group often dominates the SFG spectra.[4,5] When gauche defects are present, $CH_2$ stretch modes at the defect position become "SFG-allowed".[2−5]

SFG of adsorbates on metal and dielectric nanoparticles has been observed by several groups,[6,7] but the size dependence of the molecular conformation has not been investigated. In this work, we used gold nanoparticles of four different sizes: (1) mean diameter $\langle d \rangle = 1.8$ nm with standard deviation $\sigma_d = 1.3$ nm; (2) $\langle d \rangle = 2.9$ nm, $\sigma_d = 0.6$ nm; (3) $\langle d \rangle = 7.4$ nm, $\sigma_d = 1.1$ nm; and (4) $\langle d \rangle = 23$ nm, $\sigma_d = 8.1$ nm (Meliorum Technologies). SFG spectroscopic studies were done on submonolayer nanoparticle samples drop-cast from toluene solution onto an optical grade $CaF_2$ window. On the basis of the solution concentrations and area, the expected surface coverage is 51.8, 51.8, 721, and 14200 $nm^2$/nanoparticle for $\langle d \rangle = 1.8$ nm, 2.9, 7.4, and 23 nm samples, respectively, corresponding to 5%, 14%, 7%, and 3% of a closed-packed monolayer. Transmission electron microscopy was used to verify the size distribution and the uniform surface coverage.

A detailed description of our broadband SFG setup[5] is available in the Supporting Information section. Briefly, a broadband femtosecond infrared and a narrow-band picosecond visible (800 nm) laser pulses are spatially and temporally overlapped at the sample surface. The collected sum-frequency signal is dispersed through a monochromator onto a CCD array to obtain the SFG spectrum. The SFG signal arises because of the slight asymmetry

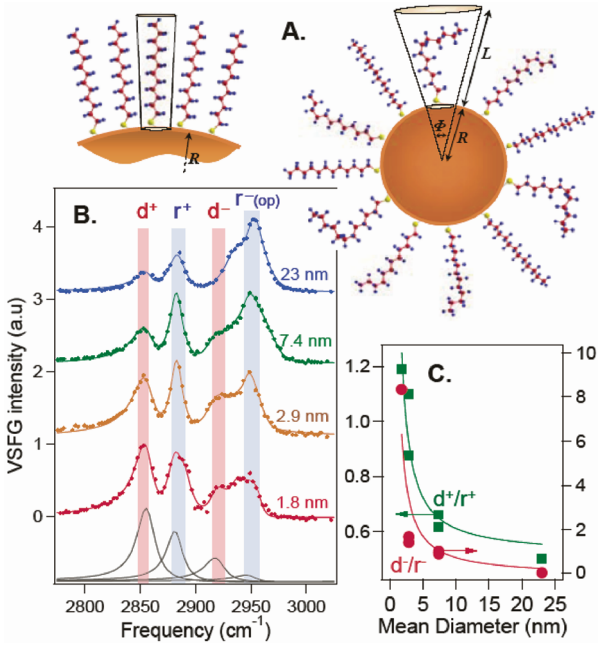


***Figure 1.*** (A) Schematic representation of the dodecanethiol ligand (chain length $L \approx 1.6$ nm) on spherical nanoparticle surfaces showing conical volume available for the formation of gauche defects; (B) size-dependent SFG spectra (SSP) of the dodecanethiol on gold nanoparticles in the CH-stretch region; (C) the ratio of the methylene ($d^+$, $d^-$) to methyl ($r^+$, $r^-$) mode intensities in the SFG spectra showing conformational change (increase of gauche defects) as a function of particle size. Solid lines show size scaling expected from the geometric increase of the conical volume available to the alkane chain on a curved surface, eq 2.

imposed by the $CaF_2$ substrate onto the physisorbed but otherwise centrosymmetric nanoparticles and is enhanced by the preresonance with the gold nanoplasmon,[6,8] similar to the Raman enhancement effect.[9] The details of the SFG enhancement effect are outside the scope of this Communication.

The SFG spectra (SSP polarization) recorded in the CH-stretch region are shown in Figure 1. The observed transitions can be readily assigned as $CH_2$ symmetric stretch ($d^+$) at 2855 $cm^{-1}$, $CH_2$ antisymmetric stretch ($d^-$) at 2918 $cm^{-1}$, $CH_3$ symmetric stretch ($r^+$) at 2881 $cm^{-1}$, and $CH_3$ asymmetric out-of-plane stretch ($r^-_{op}$) at 2950 $cm^{-1}$.[4,10] A weaker band at 2935 $cm^{-1}$ may be assigned to the Fermi resonance between $CH_3$ symmetric stretch and bend overtone modes. A clear trend is the increase of the relative intensity of the $CH_2$ versus $CH_3$ transitions with decreasing particle size. This is particularly obvious for the symmetric stretches, $d^+$ versus $r^+$, which are well separated from other modes (Figure 1B).

In order to quantify this trend, we fit the SFG spectra to a series of coherently added Lorentzian line shapes

$$I_{SFG}(\omega_{IR}) \propto \left| A_{NR} e^{i\phi} + \sum_{j=1}^{N} \frac{B_j \Gamma_j}{(\omega_{IR} - \omega_j) + i\Gamma_j} \right|^2 \qquad (1)$$



10.1021/ja065756y CCC: $33.50 

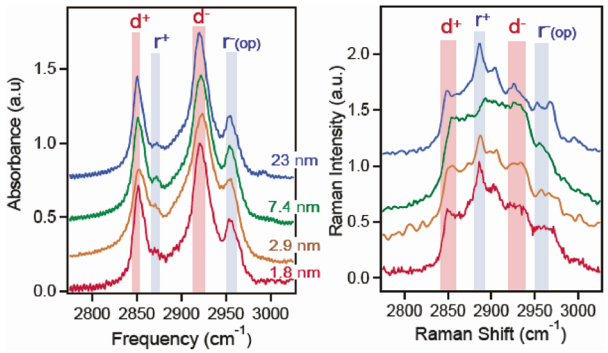


***Figure 2.*** (Left) FTIR absorption spectra; (right) spontaneous Raman spectra of dodecanethiol ligand on gold nanoparticles of four sizes.

with each vibrational mode $j$ described by amplitude $B_j$, line width $\Gamma_j$, and frequency $\omega_j$. The first term accounts for the nonresonant part of the response. Intensity of each vibrational mode is defined as $I_j \equiv |B_j|^2$. The ratio of $CH_2$ and $CH_3$ stretch intensities for the symmetric ($d^+$ to $r^+$) and asymmetric ($d^-$ to $r^-_{op}$) modes are plotted in Figure 1C as a function of mean particle diameter.

In contrast, linear (incoherent) techniques, such as FTIR absorption and spontaneous Raman, do not show systematic size-dependence of the same CH-stretch bands (Figure 2). The samples for FTIR and Raman measurements were prepared using a similar drop-casting procedure on a $CaF_2$ substrate, but were considerably thicker (multilayer) because of their inferior detection limits compared to SFG. Conformational analysis of the IR and Raman spectra often relies on the $CH_2$ vibrational frequency blue-shift of $\sim$4 to 6 $cm^{-1}$ from "solidlike" (all-trans) to "liquidlike" (gauche defects) alkane chains.[11] However, the inherently broad vibrational lines of the nanoparticle ligands (fwhm $\approx$ 15−20 $cm^{-1}$) make such analysis unreliable. We do not observe frequency shifts of more than 2 $cm^{-1}$ in any of the spectra, similar to previous FTIR studies that did not detect gauche defects even for small particles.[12]

The appearance of the $d^+$ and $d^-$ $CH_2$ modes in the SFG spectra is a clear indication of the size-dependent gauche conformational defects of the dodecanethiol ligand. Well-ordered self-assembled monolayers (SAMs) on plane gold, in which the alkyl chains are found predominantly in all-trans conformation, show the methylene modes typically less than 10% of the $CH_3$ modes.[3,4]

The relative intensity of the $d^+$ and $d^-$ $CH_2$ modes with respect to the $CH_3$ modes (Figure 1C) can be viewed as a semiquantitative measure of the extent of gauche defects in the ligand alkyl chains. A complication to this behavior may arise because of the heterogeneity of the nanoplasmon-enhanced E-field at small nanoparticles. Namely, if $CH_2$ and $CH_3$ groups are located at different average distances from the surface, their enhancement factors may be different[13] and the ratio may depend on the particle size. However, the absence of the size-dependence in the Raman spectra (Figure 2), which should have the same electromagnetic enhancement as SFG, indicates that the field heterogeneity does not affect the $CH_2$/$CH_3$ intensity ratios. Also, Raman excitation (514 nm) and Stokes (605 nm) wavelengths are much closer to the gold nanoplasmon resonance (500−530 nm) than the SFG (650 nm) and visible (800 nm), therefore the E-field enhancement and heterogeneity should be less important in the case of SFG.

A simple geometric model can be used to rationalize the observed size-dependent conformational changes. Because the trans−gauche free energy difference and the isomerization barrier are comparable to $kT$, the alkane chain is likely to entropically explore all volume available to it. On a flat surface, the cylindrical volume $V_0 = aL$ available to the chains, where $a \approx 22$ Å$^2$ is area per headgroup and $L$ is chain length, does not allow sufficient space to form gauche defects. On a curved surface of radius $R$, the chains occupy a conical segment (Figure 1A) of solid angle $\Phi = a/R^2$ between spheres of radii $R$ and $R + L$, with volume $V = (1/3)\Phi[(R + L)^3 - R^3]$. The fraction of chains with gauche conformational defects on a nanoparticle may be expected to be proportional to the additional volume relative to the cylindrical volume on a planar surface:

$$\delta(R) \propto \frac{V - V_0}{V_0} = x + \frac{1}{3}x^2 \qquad (2)$$

where $x = L/R$. Although this crude approximation omits most details of molecular structure, adsorption, shape variation, and surface defects, these geometric considerations qualitatively explain the observed size-dependence of the fraction of gauche conformation from SFG spectra, as illustrated in Figure 1C.

In conclusion, our results demonstrate the relation between the nanoscale geometry, namely the surface curvature of spherical gold nanoparticles, and the molecular conformation of the chemisorbed dodecanethiol ligand. The average thickness of the alkyl monolayer coat may therefore differ slightly from the length of the all-trans chain. This may have important implications for applications involving, for example, electron transfer, which scales exponentially with distance. Our experiments also illustrate the utility of the second-order nonlinear SFG spectroscopy as a sensitive probe of the molecular conformation, particularly for surfaces of metallic nanostructures.

**Acknowledgment.** This work is supported by the NSF CAREER Grant No. CHE-0449720. We thank the Donors of the ACS Petroleum Research Fund (Grant No. 40868-G6) for support during the initial stages of this research. We thank Prof. G. Auner and Dr. J. Smolinski of WSU Department of Electrical and Computer Engineering for their help in obtaining Raman spectra.

**Supporting Information Available:** Sample preparation; TEM images; description of the SFG setup. This material is available free of charge via the Internet at http://pubs.acs.org.

## References

(1) Shen, Y. R. *The Principles of Nonlinear Optics*; John Wiley & Sons: New York, 1984.
(2) Guyot-Sionnest, P.; Hunt, J. H.; Shen, Y. R. *Phys. Rev. Lett.* **1987**, *59*, 1597−1600.
(3) Bain, C. D. *J. Chem. Soc., Farad. Trans.* **1995**, *91*, 1281−1296.
(4) Himmelhaus, M.; Eisert, F.; Buck, M.; Grunze, M. *J. Phys. Chem. B* **2000**, *104*, 576−584. Nishi, N.; Hobara, D.; Yamamoto, M.; Kakiuchi, T. *J. Chem. Phys.* **2003**, *118*, 1904−1911.
(5) Bordenyuk, A. N.; Jayathilake, H.; Benderskii, A. V. *J. Phys. Chem. B* **2005**, *109*, 15941−15949.
(6) Kawai, T.; Neivandt, D. J.; Davies, P. B. *J. Am. Chem. Soc.* **2000**, *122*, 12031−12032. Rupprechter, G. *Phys. Chem. Chem. Phys.* **2001**, *3*, 4621−4632. Humbert, C.; Busson, B.; Abid, J. P.; Six, C.; Girault, H. H.; Tadjeddine, A. *Electrochim. Acta* **2005**, *50*, 3101−3110.
(7) Holman, J.; Ye, S.; Neivandt, D. J.; Davies, P. B. *J. Am. Chem. Soc.* **2004**, *126*, 14322−14323. Wang, C. Y.; Groenzin, H.; Shultz, M. J. *J. Phys. Chem. B* **2004**, *108*, 265−272.
(8) Baldelli, S.; Eppler, A. S.; Anderson, E.; Shen, Y. R.; Somorjai, G. A. *J. Chem. Phys.* **2000**, *113*, 5432−5438.
(9) Jiang, J.; Bosnick, K.; Maillard, M.; Brus, L. *J. Phys. Chem. B* **2003**, *107*, 9964−9972.
(10) Macphail, R. A.; Strauss, H. L.; Snyder, R. G.; Elliger, C. A. *J. Phys. Chem.* **1984**, *88*, 334−341.
(11) Hostetler, M. J.; Stokes, J. J.; Murray, R. W. *Langmuir* **1996**, *12*, 3604−3612. Bryant, M. A.; Pemberton, J. E. *J. Am. Chem. Soc.* **1991**, *113*, 3629−3637.
(12) Shimizu, T.; Teranishi, T.; Hasegawa, S.; Miyake, M. *J. Phys. Chem. B* **2003**, *107*, 2719−2724. Badia, A.; Cuccia, L.; Demers, L.; Morin, F.; Lennox, R. B. *J. Am. Chem. Soc.* **1997**, *119*, 2682−2692. Ang, T. P.; Wee, T. S. A.; Chin, W. S. *J. Phys. Chem. B* **2004**, *108*, 11001−11010.
(13) Compagnini, G.; Galati, C.; Pignataro, S. *Phys. Chem. Chem. Phys.* **1999**, *1*, 2351−2353.

JA065756Y